

Discovery of Novel Irreversible HER2 Inhibitors for Breast Cancer Treatment

Jhih-Yan Tang^{1*}, Yih Ho^{2*}, Chun-Yi Chang³, Hsuan-Liang Liu^{1,3} 

¹Department of Chemical Engineering and Biotechnology, National Taipei University of Technology, Taiwan;

²School of Pharmacy, College of Pharmacy, Taipei Medical University, Taiwan; ³Institute of Biochemical and Biomedical Engineering, National Taipei University of Technology, Taiwan

Correspondence to: Hsuan-Liang Liu, f10894@ntut.edu.tw

Keywords: Breast Cancer, Irreversible HER2 Inhibitors, Structure-Based Pharmacophore Modeling, Molecular Docking, Molecular Dynamics Simulation

Received: March 15, 2019

Accepted: April 19, 2019

Published: April 22, 2019

Copyright © 2019 by authors and Scientific Research Publishing Inc.

This work is licensed under the Creative Commons Attribution International License (CC BY 4.0).

<http://creativecommons.org/licenses/by/4.0/>



Open Access

ABSTRACT

It has been widely known that human epidermal growth factor receptor 2 (HER2) inhibitors exhibit distinct antitumor responses against HER2-positive breast cancer. To date, Lapatinib (Tykerb[®]) has been approved by the U.S. Food and Drug Administration (FDA) as a reversible HER2 inhibitor for treating breast cancer. However, HER2 L755S, T798I and T798M mutations confer drug resistance to lapatinib, restricting its efficacy toward HER2-positive breast cancer. Thus, novel therapy toward mutant HER2 is highly desired. Although several irreversible HER2 inhibitors have been developed to overcome these drug resistance problems, most of them were reported to cause severe side effects. In this study, three pharmacophore models based on HER2 L755S, T798I and T798M mutant structures were constructed and then validated through receiver operating characteristic (ROC) curve analysis and Güner-Henry (GH) scoring methods. Subsequently, these well-validated models were utilized as 3D queries to identify novel irreversible HER2 inhibitors from National Cancer Institute (NCI) database. Finally, two potential irreversible HER2 inhibitor candidates, NSC278329 and NSC718305, were identified and validated through molecular docking, molecular dynamics (MD) simulations and ADMET prediction. Furthermore, the analyses of binding modes showed that both NSC278329 and NSC718305 exhibit good binding interactions with HER2 L755S, T798I and T798M mutants. All together, the above results suggest that both NSC278329 and NSC718305 can serve as novel and effective irreversible HER2 inhibitors for treating breast cancers with HER2 L755S, T798I and T798M mutants. In addition, they may act as lead compounds for designing new irreversible HER2 inhibitors

*Equal contribution.

by carrying out structural modifications and optimizations in future studies.

1. INTRODUCTION

The World Health Organization (WHO) reports that breast cancer is one of the most common malignancies among women worldwide [1]. Due to its complexity, the therapies of breast cancer can be very different in various patients. Human epidermal growth factor receptor 2 (HER2), a member of the ErbB family, is involved in the signal transduction pathways, leading to cell growth and proliferation. Clinically, HER2 amplification or overexpression has been reported in 30% of breast cancers and is correlated with poor prognosis, increased metastatic potential and resistance to apoptosis [2, 3]. Therefore, blocking of HER2 has been considered as an effective strategy for breast cancer therapy [4].

However, the efficacy of several anti-HER2 therapeutics, such as small molecule HER2 tyrosine kinase inhibitors (TKIs), is limited by the occurrence of several HER2 point mutations, such as L755S, T798I and T798M [5]. These mutations have been reported to drive rapid development of solid tumors that exhibit strong resistance to a variety of TKIs, including the FDA-approved agent lapatinib (Tykerb®), a reversible HER2 inhibitor that is clinically used for the treatment of late-stage breast cancer [6]. Previous studies have shown that both irreversible epidermal growth factor receptor (EGFR) inhibitors, neratinib (HKI-272) [7] and afatinib (BIBW-2992) [8], are effective for the treatment of lung cancer with EGFR T790M point mutation [9]. Recent studies also provide compelling evidence indicating that these irreversible EGFR inhibitors were able to inhibit breast cancer cells expressing HER2 L755S, T798I and T798M point mutations [10, 11]. The major difference between reversible and irreversible HER2 inhibitors is that irreversible HER2 inhibitors have α , β -unsaturated carbonyl substructures, which are also known as “Michael acceptors”. With these Michael acceptors, irreversible HER2 inhibitors are able to form carbon-sulfur bond between the β -carbon of the Michael acceptors and the sulfhydryl groups of the HER2 Cys805 residue through Michael addition [12, 13]. The formation of this covalent bond allows these irreversible HER2 inhibitors to overcome drug resistance caused by HER2 point mutations. However, several severe side effects, such as liver damage and diarrhea, limit the clinical uses of both neratinib and afatinib [14]. Therefore, it is highly desired to discover novel irreversible HER2 inhibitors for the treatment of breast cancer expressing HER2 L755S, T798I and T798M point mutations.

So far, due to the lack of HER2 L755S, T798I and T798M mutant structures, the strategies to develop novel irreversible HER2 inhibitors were limited to experimental methods, such as lead modification, enzyme inhibitory analysis, and cell proliferation assay [15]. Although several irreversible HER2 inhibitors have been synthesized and analyzed *in vitro* or *in vivo*, their binding modes and efficacy against HER2 L755S, T798I and T798M mutants are still unknown. In this study, we aimed to discover novel irreversible HER2 inhibitors targeting HER2 L755S, T798I and T798M point mutations from the National Cancer Institute (NCI) database by a combination of several computational approaches, such as homology modeling, structure-based pharmacophore modeling, virtual screening, molecular docking, molecular dynamics (MD) simulations and ADMET (absorption, distribution, metabolism, excretion, and toxicity) prediction. Finally, the selected irreversible HER2 inhibitors can be further tested *in vitro/in vivo* and provide important information for designing better irreversible HER2 inhibitors for clinical uses. The aim of this study is to discover potential irreversible HER2 inhibitors with stronger efficacy and better ADMET properties through a combination of several computational approaches and the entire concept of this study is illustrated in Figure 1. To the best of our knowledge, this is the first attempt to apply structure-based approach to discovery potent irreversible HER2 inhibitors with novel structural scaffolds and desired chemical features for treating breast cancer with HER2 L755S, T798I and T798M mutants.

2. MATERIALS AND METHODS

2.1. Protein and Ligand Preparation

The crystal structure of wild-type HER2-TAK285 (PDB ID: 3RCD; resolution: 3.21Å) was obtained

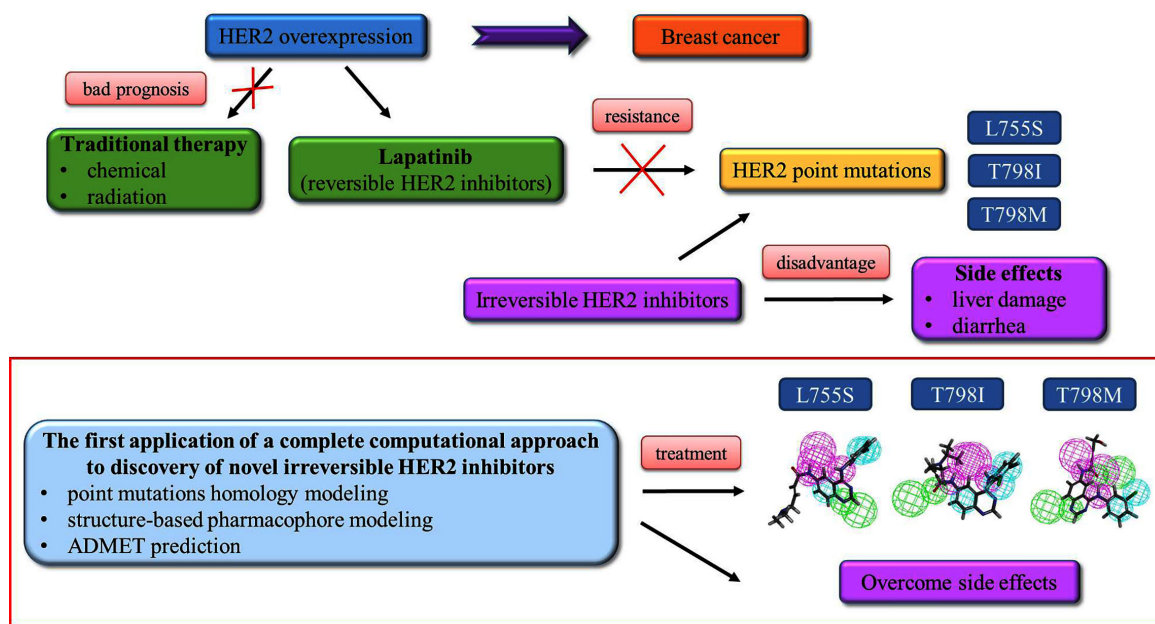


Figure 1. Schematic overview of this study. HER2 overexpression leads to breast cancer, which may be treated by traditional therapies or lapatinib, a reversible HER2 inhibitor. However, several HER2 point mutations, such as L755S, T798I, and T798M, exhibit resistance to lapatinib. Current HER2 irreversible inhibitors cause many severe side effects. The aim of this study is to discover potential irreversible HER2 inhibitors with stronger efficacy and better ADMET properties through a combination of several computational approaches.

from the RCSB Protein Data Bank and prepared using “Prepare Protein” algorithm of Discovery Studio 2017 (DS2017). Using the “Define Site” tool of DS2017, the active site of HER2 structure was defined as a collection of several critical residues, such as Leu755, Thr798, and Cys805 etc., enclosed within a sphere of 11 Å radius around the co-crystallized ligand TAK285. Then, the co-crystallized ligand TAK285 and crystal water molecules were removed and only the wild-type HER2 structure was retained as the target template. Based on the structure of wild-type HER2, the structures of HER2 L755S, T798I and T798M mutants were constructed using the “Build Mutant” option implemented in DS2017. Subsequently, the qualities of these HER2 mutant structures were evaluated by the on-line UCLA SAVES server. All the HER2 mutant structures showed only 0.4% of residues in the disallowed region (Figure 2), which indicates that these constructed mutant structures have reasonable and stable conformations for the subsequent pharmacophore modeling. For active ligands, 40 known irreversible HER2 inhibitors were collected from previous literatures [16, 17]. Their 3D structures were built using the sketch function of DS2017 and then optimized using “Prepare Ligand” algorithm. These 40 irreversible HER2 inhibitors, as shown in Figure 3, were named as compounds 1-40 according to their IC_{50} (from the lowest to the highest).

2.2. Structure-Based Pharmacophore Model Generation and Validation

Due to the lack of receptor-ligand binding information, each of the known 40 irreversible HER2 inhibitors was individually docked into the active sites of HER2 L755S, T798I and T798M mutant structures and a maximum of 10 binding poses were generated for each receptor-ligand complex using CDOCKER. For each receptor-ligand complex, the generated docking pose with the best CDOCKER interaction energy was selected for pharmacophore modeling. Thus, a total of 120 docking poses were selected for the generation of structure-based pharmacophore models using the “Receptor-Ligand Pharmacophore Generation” protocol of DS2017 [18, 19]. For each receptor-ligand binding complex, a maximum of 10 pharmacophore

models with 4-6 pharmacophore features were automatically generated with default parameters. Finally, a total of 36, 36, and 38 pharmacophore models based on HER2 L755S, T798I, and T798M mutant structures were constructed, respectively.

To select the best structure-based pharmacophore models for HER2 L755S, T798I, and T798M mutant, a test 3D database comprising both 40 known irreversible HER2 inhibitors and 254 decoys (from DecoyFinder-2.0) was constructed using “Build 3D Database” (maximum 255 conformations for each compound) of DS2017. Then, the constructed pharmacophore models were used for screening the test 3D database using “Screen Library” program of DS2017 with default parameters. Subsequently, Güner-Henry (GH) scoring and receiver operating characteristic (ROC) analysis methods were adopted to evaluate the screening results of each model. Finally, three models (named as models I, II and III), which were constructed based on the HER2 L755S-compound **39**, HER2 T798I-compound **10** and HER2 T798M-compound **6** complexes, respectively, displayed the best GH scores and “excellent” ROC curves and were selected for further virtual screening.

2.3. Virtual Screening

The flowchart of the overall virtual screening procedure in this study is summarized in **Figure 4**. First, the NCI database were downloaded and filtered by both Lipinski’s rule-of-five [20] and Veber’s rule [21] to enhance the drug-like properties of the screening results [22]. Then, models I, II, and III were used as 3D search queries to identify novel irreversible HER2 inhibitors using “Screen Library” protocol of DS2017 with default parameters. To segregate irreversible HER2 inhibitors from the reversible ones, only compounds with Michael acceptors were selected by visual inspection. Finally, a total of 143, 72 and 191

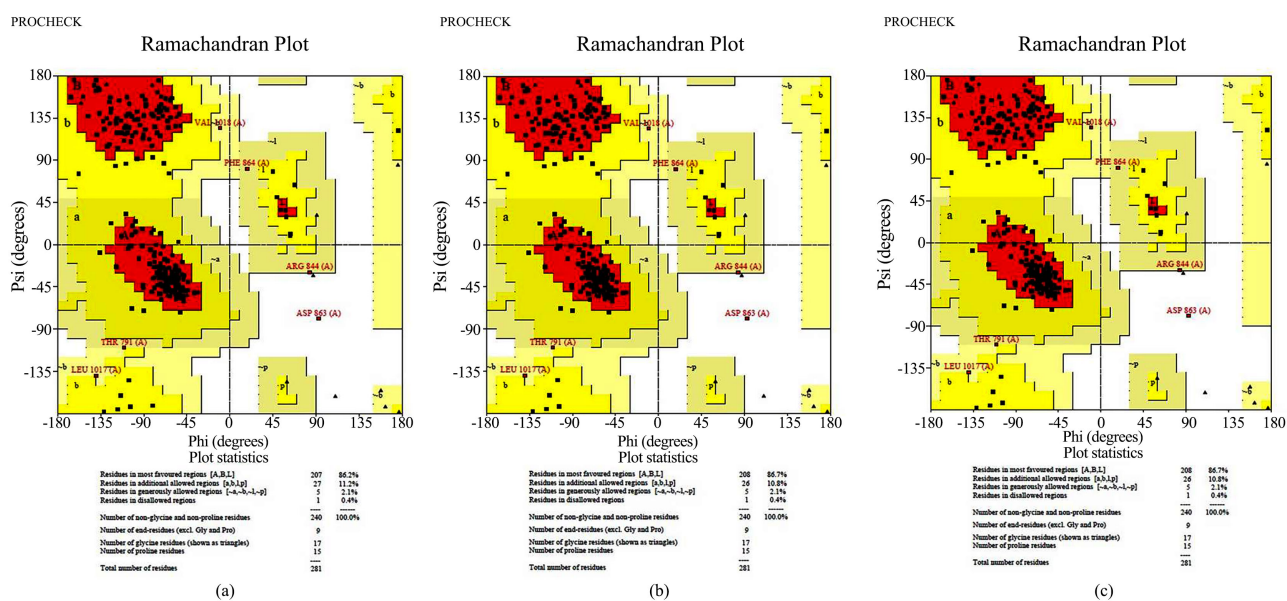


Figure 2. Ramachandran plot analysis of the constructed mutant structures. The different colored areas indicate “disallowed” (white), “generously allowed” (beige), “additional allowed” (yellow), and “most favored” (red) regions. (a) For HER2 L755S mutant, approximately 86.2% of amino acid residues are in the most favored regions, 11.2% in the additional allowed regions, 2.1% in the generally allowed regions and 0.4% in the disallowed region; (b) For HER2 T798I mutant, approximately 86.7% of amino acid residues are in the most favored regions, 10.8% in the additional allowed regions, 2.1% in the generally allowed regions and 0.4% in the disallowed region; (c) For HER2 T798M mutant, approximately 86.7% of amino acid residues are in the most favored regions, 10.8% in the additional allowed regions, 2.1% in the generally allowed regions and 0.4% in the disallowed region.

compounds were selected from models I, II, and III, respectively, as potential irreversible HER2 inhibitors for the further molecular docking studies (Figure 4).

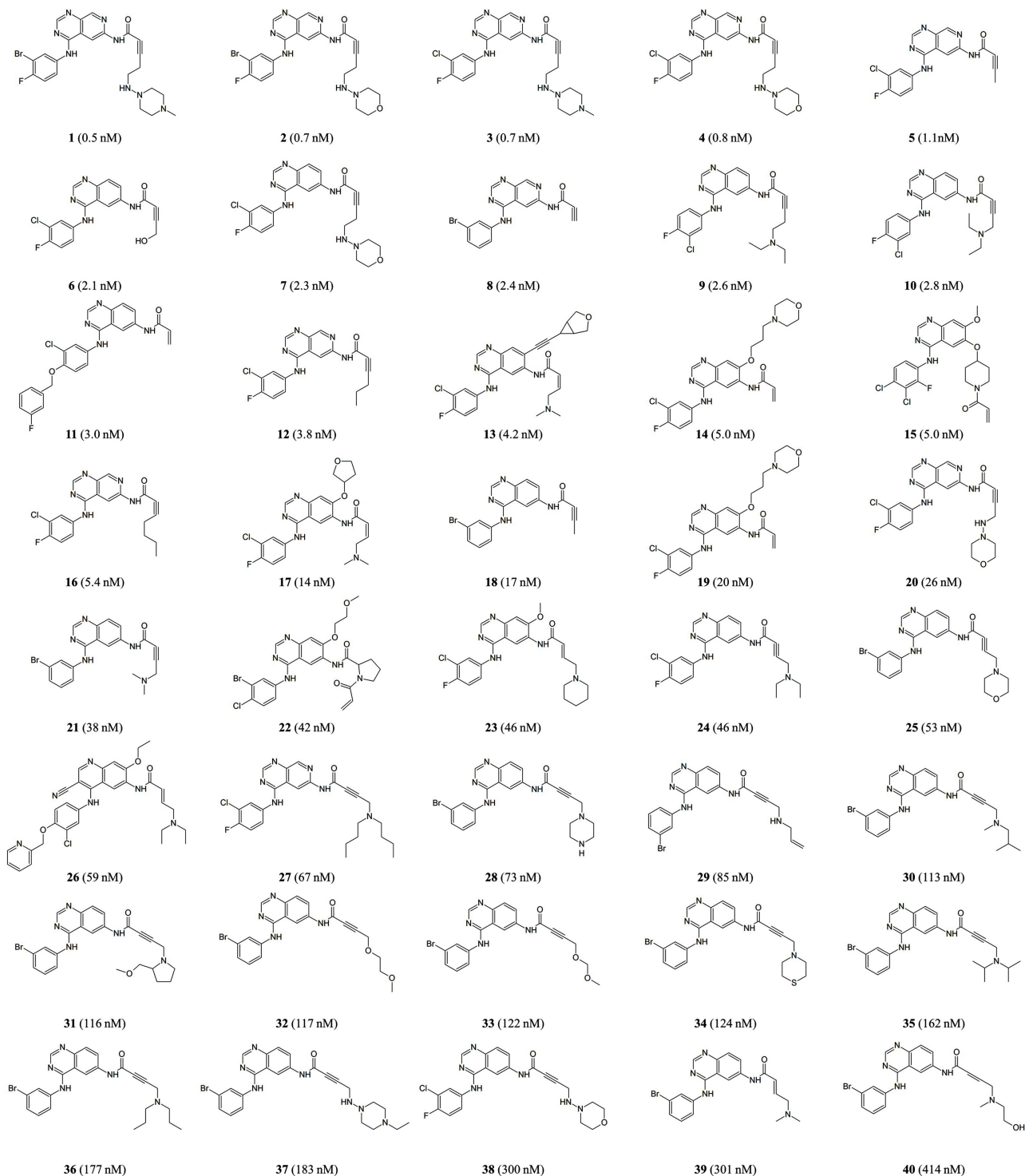


Figure 3. 2D structures and biological activities (IC_{50} values, nM) of the 40 known irreversible HER2 inhibitors selected on the basis of their affinities toward HER2 inhibitory from the highest to the lowest.

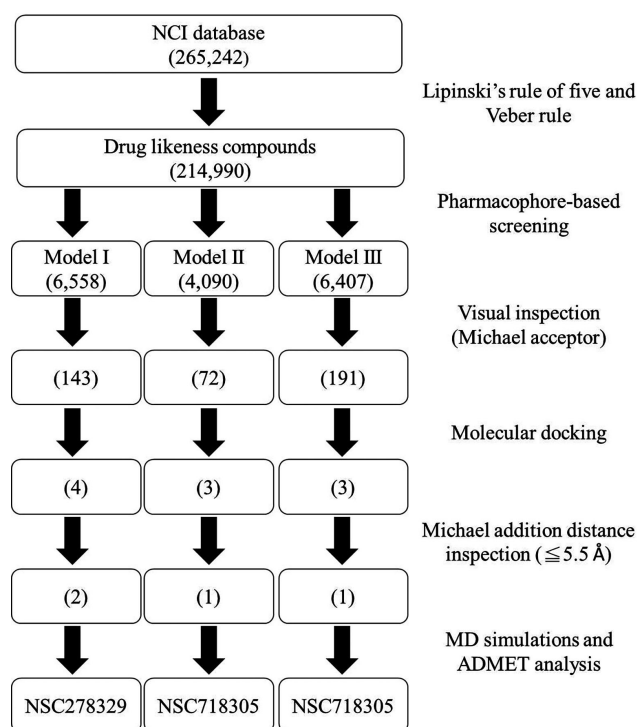


Figure 4. The overall workflow depicting different stages of virtual screening in this study.

2.4. Molecular Docking

The selected 143, 72 and 191 potential irreversible HER2 inhibitors were separately docked into the active sites of HER2 L755S, T798I and T798M mutant structures, respectively, using the CDOCKER program of DS2017 with CHARMM force field. Subsequently, the CDOCKER interaction energies ($\text{kcal}\cdot\text{mol}^{-1}$), which are also known as CDOCKER scores, were obtained from these docking studies. These docking results were further compared to those of the 40 known irreversible HER2 inhibitors, including HER2 L755S-compound **22**, HER2 T798I-compound **14** and HER2 T798M-compound **19**. These complexes displayed the lowest CDOCKER interaction energies among all of the 40 known irreversible HER2 inhibitors. Finally, the ones which exhibited lower CDOCKER interaction energies than those known irreversible HER2 inhibitors were selected as hit compounds.

In order to investigate the binding conformations in the active sites of the HER2 mutants, the selected hit compounds were subjected to further visual inspection based on the main criteria that the distance between Michael acceptors of each selected compound and the sulfhydryl group of HER2 Cys805 must be within the ideal range (5.5 \AA) for Michael addition [23]. Finally, compounds with better binding affinity and favorable binding poses for Michael addition were retrieved as potential irreversible HER2 inhibitors.

2.5. Molecular Dynamics (MD) Simulations

MD simulations were performed to confirm the binding stabilities of the selected potential irreversible HER2 inhibitors using the Gromacs 2016.3 software package [24, 25]. With Amber Tools 2017, the AMBER99SB-ILDN force field [26] was assigned for proteins and the general AMBER force field (GAFF) was assigned for ligands [27, 28]. In a 10.0 \AA dodecahedron periodic box, the system was solvated with TIP3P water model and neutralized by replacing solvent molecules with counter ions. Subsequently, the entire system was stabilized through energy minimization and the equilibration of each system was conducted at constant volume (NVT) for 200 ps and constant pressure (NPT) for 200 ps. Finally, the equilibrated systems were subjected to 50 ns production runs at constant temperature (300 K) and pressure (1 atm).

2.6. ADMET Analysis

ADMET properties of the selected potential irreversible HER2 inhibitors were obtained by uploading the simplified molecular input line entry specification (SMILES) data of each compound to the online webserver admetSAR [29]. In this webserver, mathematical models (human intestinal absorption, CYP450 inhibition, hERG inhibition, AMES toxicity and Carcinogenicity) were used to quantitatively predict the properties of a set of rules that specify ADMET characteristics of the chemical structures for the selected potential irreversible HER2 inhibitors. Compounds with satisfactory ADMET properties were finally selected as safe and novel irreversible HER2 inhibitors for breast cancer treatment.

3. RESULTS AND DISCUSSION

In the past decades, lapatinib has been used as an effective reversible HER2 inhibitor for the treatment of HER2-positive breast cancers. However, HER2 L755S, T798I and T798M point mutations have been reported to drive resistance toward lapatinib, thus restricting its clinical uses. Previous studies have indicated that irreversible HER2 inhibitors were able to form covalent bonds with these HER2 mutant structures through Michael addition, thus can overcome the resistance caused by these HER2 mutations. However, most of the known irreversible HER2 inhibitors were reported to cause lethal side effects due to bad ADMET properties. Therefore, there was a desire for developing novel irreversible HER2 inhibitors which are safe and potent. In this study, homology modeling, structure-based pharmacophore modeling, virtual screening, molecular docking, MD simulations and ADMET analysis were combined to discover novel irreversible HER2 inhibitors targeting HER2 L755S, T798I and T798M mutants. To the best of our knowledge, this is the first attempt to utilize structure-based approach to discover potent irreversible HER2 inhibitors with novel structural scaffolds and desired chemical features for treating breast cancer with HER2 L755S, T798I and T798M mutants.

3.1. Structure-Based Pharmacophore Model Generation and Validation

Structure-based pharmacophore models are generated from the structures of the protein-ligand complexes through investigating the important interactions and excluded volumes in their binding sites [30]. Comparing to ligand-based approach, structure-based approaches have advantages of more precise prediction, good filter to remove decoys and finding structurally novel ligands against target receptors [31]. To date, the X-ray crystallographic structures of HER2 L755S, T798I and T798M mutants have not yet been reported. In order to carry out structure-based pharmacophore modeling, the homology models of HER2 L755S, T798I and T798M mutants were generated from the wild-type HER2 structure (PDB ID: 3RCD) using “Build Mutant” protocol and validated by Ramachandran plot.

To obtain receptor-ligand docking poses, 40 known irreversible HER2 inhibitors were individually docked into the constructed HER2 L755S, T798I and T798M mutant structures using CDOCKER protocol. Then, the generated 120 docking complexes were applied to structure-based pharmacophore modeling, and a total of 36, 36, and 38 models based on HER2 L755S, T798I, and T798M mutant structures were constructed, respectively. Then, the performance of these models was further validated by GH scoring method and ROC analysis [32-35].

For HER2 L755S mutant, the optimal structure-based pharmacophore models (model I) was constructed based on the HER2 L755S-compound **39** complex (Figure 5(a)). Compound **39** displays hydrogen bonding interactions with Lys753, Thr862 and Asp863 in the active site of HER2 L755S mutant, which have been identified as critical residues for HER2 inhibitory. Based on the HER2 L755S-compound **39** complex, model I contains three hydrophobic (HY) features, one hydrogen bond acceptor (HA) anchoring the ligand with Lys753, and two hydrogen bond donors (HD) anchoring the ligand with Thr862 and Asp863 (Figure 5(d)). As shown in Table 1, model I can successfully recognize 39 out of 40 known irreversible HER2 inhibitors (sensitivity = 0.975) and correctly exclude 241 out of 254 decoys (specificity = 0.949). In addition, model I possess the best GH scores of 0.77 (Table 1) and excellent ROC curve with

AUC values of 0.98, demonstrating that the quality of model I is acceptable for further virtual screening [36].

For HER2 T798I mutant, the optimal structure-based pharmacophore model (model II) was constructed from HER2 T798I-compound 10 complex (Figure 5(b)). Compound 10 forms hydrogen bonds with two important residues, Cys805 and Asp863. Based on the HER2 T798I-compound 10 complex, model II consists of three HY features, one HA with Cys805 and two HDs with Asp863 (Figure 5(e)). As shown in Table 1, model II can recognize 39 out of 40 known irreversible HER2 inhibitors (sensitivity = 0.975) and exclude 246 out of 254 decoys (specificity = 0.969). Besides, model II possess the best GH scores of 0.84 (Table 1) and excellent ROC curve with AUC values of 0.980, indicating that the quality of model II is acceptable for the subsequent virtual screening.

For HER2 T798M mutant, the optimal structure-based pharmacophore model was built from the HER2 T798M-compound 6 complex (Figure 5(c)). Unlike HER2 T798I mutant, the sulfur group of Met798 and the 3-chloro-4-fluoroaniline substituent group of compound 6 bound with each other through S/ π interaction, which has been identified as prevalent and important stabilizing interaction [37]. Such interaction can twist the binding conformation of compound 6 in the HER2 T798M mutant. Meanwhile, the nitrogen atom of pyrimidine ring forms a hydrogen bond with Cys805 and the carbonyl substructure forms hydrogen bond with Lys753. Based on such binding conformation, the generated model III consists of two HY features, two HAs with Lys753 and Cys805, and two HDs with Asn850 and Asp863 (Figure 5(f)). As shown in Table 1, model III can successfully recognize 39 out of 40 known irreversible HER2 inhibitors (sensitivity = 0.975) and exclude 242 out of 254 decoys (specificity = 0.953). Furthermore, model III possess the best GH scores of 0.79 (Table 1) and excellent ROC curve with AUC values of 0.983, suggesting that the quality of model III is good enough for further virtual screening. The above validation results all confirm that models I-III exhibit high predictive efficiency and can be served as reliable 3D queries for the further virtual screening procedures [38].

Table 1. The evaluation of pharmacophore model I (derived from HER2 L755S-compound 39 complex), model II (derived from HER2 T798I-compound 10 complex) and model III (derived from HER2 T798M-compound6 complex) based on Güner-Henry (GH) scoring method.

Parameter	Model I	Model II	Model III
Total molecules in database (D)	294	294	294
Total number of actives in database (A)	40	40	40
Total number of hit molecules from database (Ht)	52	47	50
Total number of active molecules in hit list (Ha)	39	39	39
% yield of actives (%Y) [(Ha/Ht) × 100]	75.00	82.98	78.00
% ratio of actives (%A) [(Ha/A) × 100]	97.50	97.50	97.50
False negatives [A-Ha]	1	1	1
False positives [Ht-Ha]	13	8	11
Enrichment factor (EF) [(Ha × D)/(Ht × A)]	5.14	5.68	5.34
Goodness of hit score (GH) ^a	0.77	0.84	0.79

D is number of compounds in a database, A is the number of active compounds in the database, Ht is the number of hits retrieved, Ha is the number of actives in hit list, %Y is the fraction of hit relative to the size of database (hit rate or selectivity), %A is the ratio of actives retrieved in hit list, EF is the enrichment of active bin by model relative to random screening, GH is the Güner-Henry score.

$$^a \left[\left(\frac{Ha}{4Ht \times A} \right) (3A + Ht) \times \left(1 - \left(\frac{Ht - Ha}{D - A} \right) \right) \right]; \text{ GH score } > 0.7 \text{ indicates a statistically good model.}$$

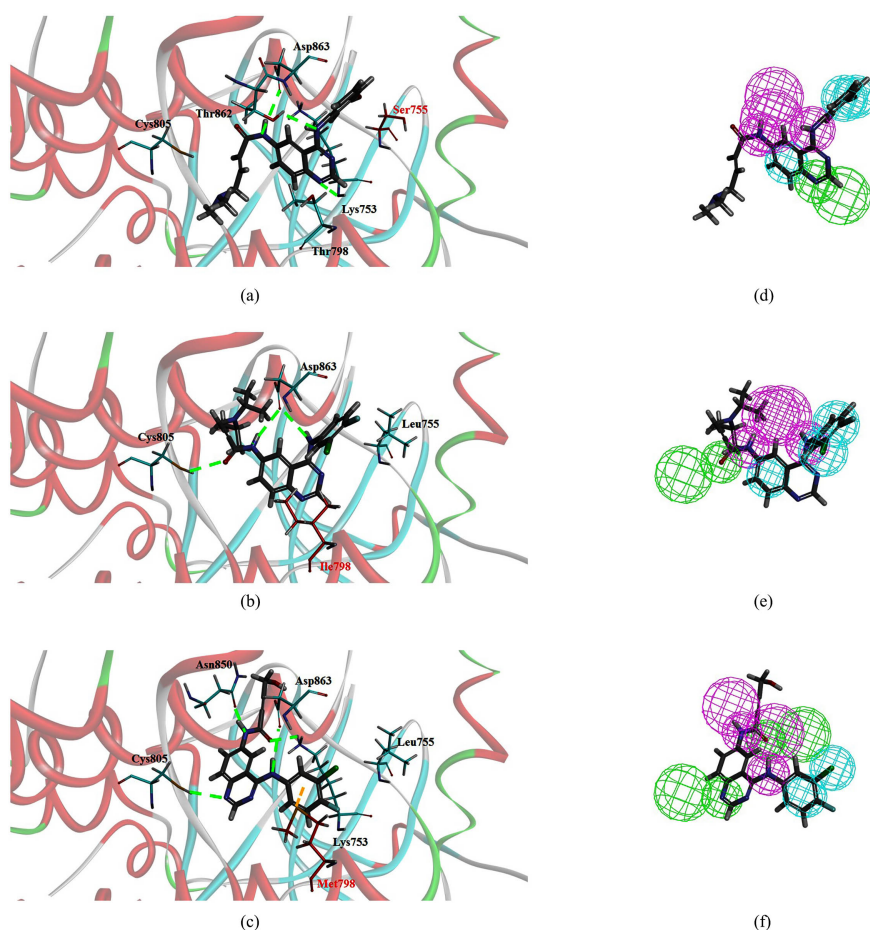


Figure 5. The docking conformations of (a) HER2 L755S-compound 39, (b) HER2 T798I-compound 10, and (c) HER2 T798M-compound 6 complexes and the developed structure-based pharmacophore models of (d) model I, (e) model II and (f) model III. For each complex, the green dashed lines represent hydrogen bonds and the yellow dashed lines represent S/ π interactions. Furthermore, each model was composed of HBA (green), HBD (purple) and HY (blue) features. For clarity of display, the excluded volumes are not included.

In order to investigate the influence caused by point mutation, compounds 6, 10, 39 were docked into the active sites of WT HER2 structure. Then the docking conformations were compared with those of HER2 mutants. As shown in **Figure 6(a)**, the residues of WT HER2 and HER2 L755S mutant were almost overlapped; therefore, compound 39 displayed similar docking conformations in both binding sites of WT HER2 and HER2 L755S mutant. The results suggest that compound 39 is a very good irreversible HER2 inhibitor for both WT HER2 and HER2 L755S mutant. As shown in **Figure 6(b)**, Met798 residue is bulkier than Thr798, which caused slight steric collision for compound 10, leading to moving upward to reduce such steric collision. As for the docking poses of compound 6, T798M mutation also caused critical steric collision to the ligand, resulting in breaking the hydrogen bond between compound 6 and Met801 residue, which further caused the different binding conformations for WT HER2 and HER2 T798M mutant (**Figure 6(c)**).

3.2. Virtual Screening and Molecular Docking

Virtual screening is a versatile technique to identify novel and potent lead compound for particular

drug target [39]. In order to identify novel irreversible HER2 inhibitors, NCI database (265,242 compounds) was utilized for our virtual screening and the flowchart is shown in Figure 4. For primary screening, all compounds were filtered with Lipinski's rule-of-five and Veber's rule to obtain the drug-like compounds. Then the optimal pharmacophore models I-III were used as 3D queries to screen the newly drug-like compounds library with the best search mode to discover the novel scaffold of HER2 inhibitors. Subsequently, visual inspection was carried out to retrieved potential irreversible HER2 inhibitors with Michael acceptors, which are essential to form covalent interactions with HER2 mutants. Finally, these potential irreversible HER2 inhibitors were subjected to further docking studies to investigate their binding conformations.

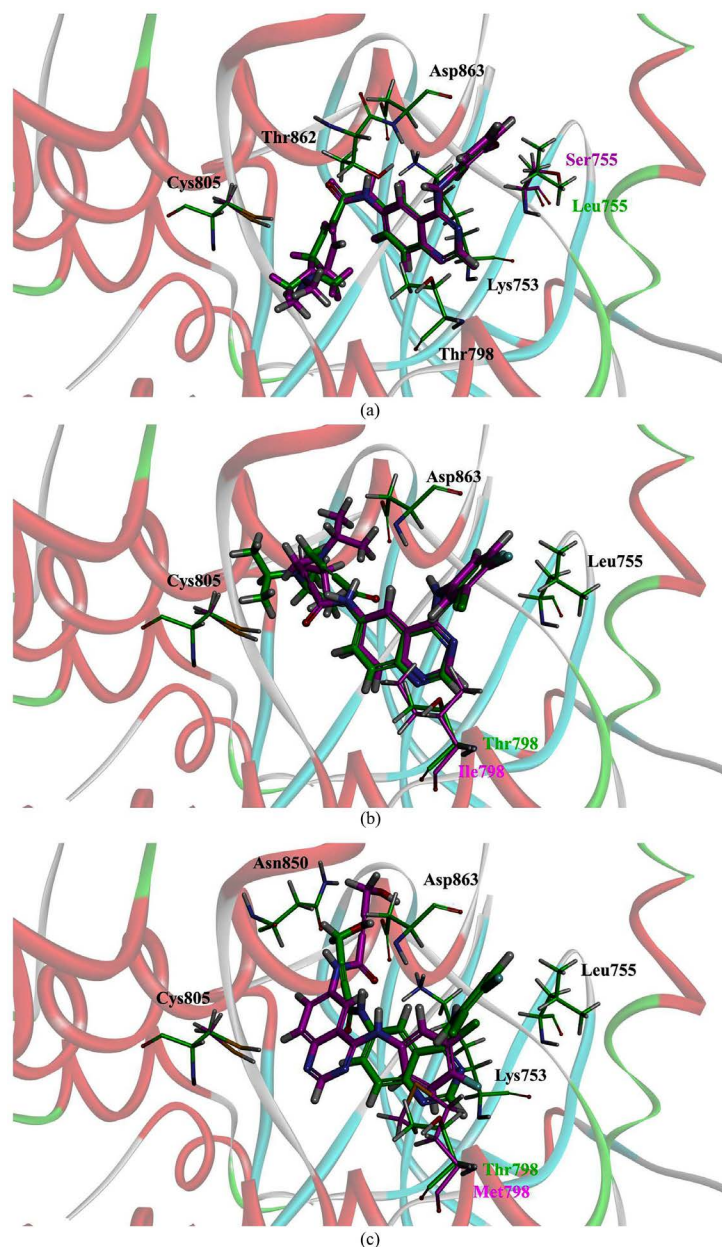


Figure 6. Docking conformations of (a) compound 39, (b) compound 10, and (c) compound 6 toward HER2 WT and HER2 mutants. Conformations based on WT HER2 were represented by green sticks, and the complexes based on mutant HER2 were represented by purple sticks.

Molecular docking is a well-established method to predict the molecular-level interactions of small molecules in the receptor active sites. In order to investigate the binding interactions between receptors and ligands, these potential irreversible HER2 inhibitors were individually docked into the active sites of HER2 L755S, T798I and T798M mutant structures and CDOCKER interaction energies ($\text{kcal}\cdot\text{mol}^{-1}$) obtained in the docking experiments were utilized to evaluate their binding interactions as presented in **Table 2**. For HER2 L755S mutant, compound **22**, which showed the lowest CDOCKER interaction energies of -61.859 kcal/mol, was the optimal compound among 40 known irreversible HER2 inhibitors. Among the selected 143 compounds, NSC278329 (-62.748 kcal/mol), NSC381866 (-65.115 kcal/mol), NSC642003 (-63.009 kcal/mol) and NSC659397 (-62.345 kcal/mol) showed lower CDOCKER interaction energies than that of compound **22**, thus were considered to exhibit stronger binding interactions. In addition to the docking scores, the essential covalent interactions of these docking complexes were also predicted by measuring the distances between the Michael acceptors of the inhibitors and the Cys805 residues of HER2 L755S mutant. According to previous literature, the distance for Michael addition should be within the ideal range of 5.5 Å. Among these binding complexes, the distances were 5.0 Å for NSC278329 and 4.5 Å for NSC642003 (**Figure 7(a)** and **Figure 7(b)**). Therefore, we anticipated that only NSC278329 and NSC642003 can execute Michael addition by forming covalent bonds between their Michael acceptors and the sulfhydryl group of Cys805 in HER2 L755S mutant. In addition, NSC278329 displayed strong hydrogen bonding interactions with Ala730, Lys753, Thr862, Asp863 and hydrophobic interactions with Val734, Leu796, Cys805 residues in the active site of HER2 L755S mutant (**Figure 8(a)**). NSC642003 formed hydrogen bonding interactions with Lys753, Asn850, Asp863 and hydrophobic interactions with Leu726, Ala751, Met774, Leu785, Leu796, Leu800, Cys805, Leu852, Phe864, Phe1004 in the HER2 L755S mutant (**Figure 8(b)**). All together, the above results suggest that both of NSC278329 and NSC642003 were in the vicinity of the active site containing the critical residues, such as Leu726, Gly729, Val734, Ala751, Lys753, Cys805, Arg849, Leu852, Thr862, Asp863. Finally, HER2 L755S-NSC278329, HER2 L755S-NSC642003 docking complexes were subjected for MD simulations to estimate their binding stabilities.

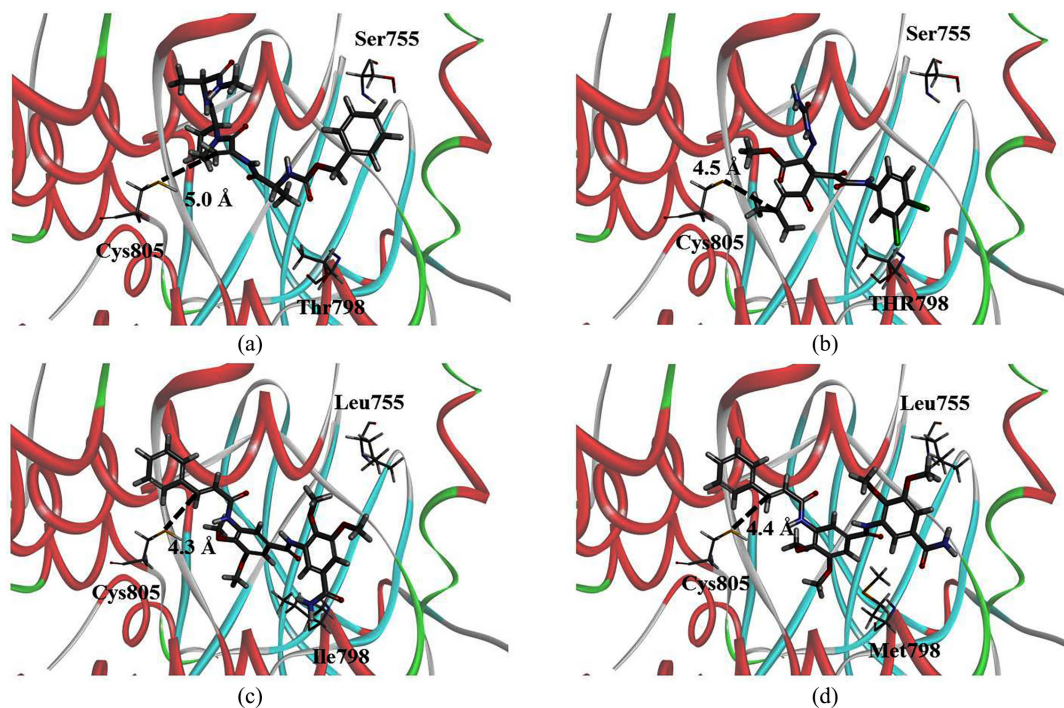


Figure 7. Docking poses of (a) HER2 L755S-NSC278329, (b) HER2 L755S-NSC642003, (c) HER2 T798I-NSC718305 and (d) HER2 T798M-NSC718305. The dashed line represents the distances between the residue Cys805 of HER2 mutants and the Michael acceptors of each inhibitor.

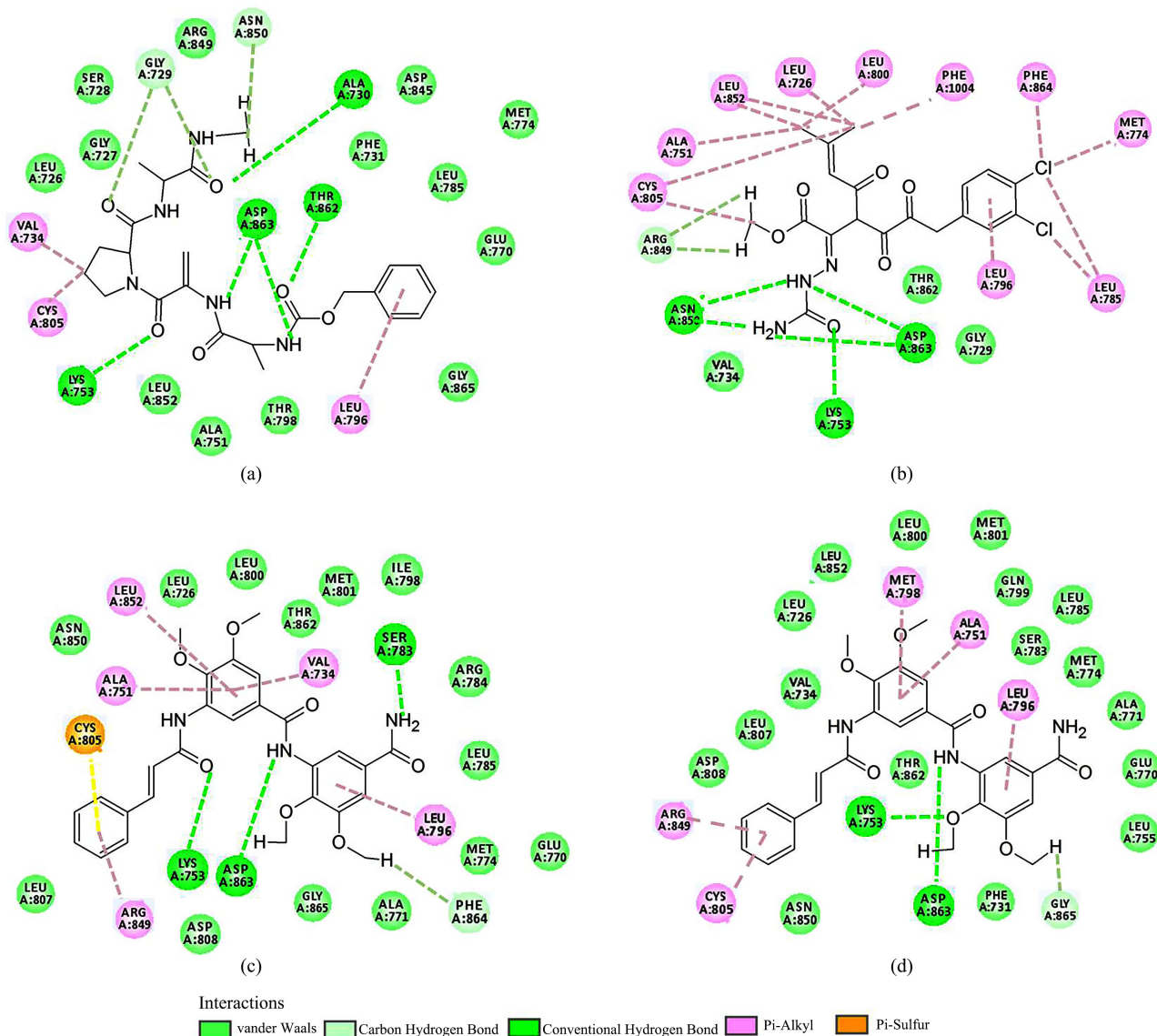


Figure 8. 2D interaction diagrams for (a) HER2 L755S-NSC278329, (b) L755S-NSC642003, (c) HER2 T798I-NSC718305 and (d) HER2 T798M-NSC718305.

Table 2. CDOCKER scores (kcal/mol) of each screened compound and the known irreversible HER2 inhibitors.

HER2 L755S		HER2 T798I		HER2 T798M	
Compounds	CDOCKER scores	Compounds	CDOCKER scores	Compounds	CDOCKER scores
22	-61.859	14	-59.644	19	-59.719
NSC278329	-62.748	NSC702108	-60.981	NSC659505	-60.220
NSC381866	-65.115	NSC702137	-60.748	NSC692910	-59.838
NSC642003	-63.099	NSC718305	-68.817	NSC718305	-66.841
NSC659397	-62.345				

When docking to the HER2 T798I mutant structure, NSC702108 (−60.981 kcal/mol), NSC702137 (−60.748 kcal/mol) and NSC718305 (−68.817 kcal/mol) all had lower CDOCKER interaction energies than the optimal known irreversible HER2 inhibitor compound **14** (−59.644 kcal/mol) (Table 2). Based on their docking results, these compounds with lower CDOCKER interaction energies were considered to exhibit stronger binding interactions than all of the 40 known irreversible HER2 inhibitors, thus were retrieved for further visual inspection. The distance between Michael acceptor of NSC718305 and Cys805 of HER2 T798I mutant was about 4.3 Å, indicating that NSC718305 can execute Michael addition by forming covalent bond between their Michael acceptors and the sulfhydryl group of Cys805 in HER2 T798I mutant (Figure 7(c)). However, NSC702108 and NSC702137 did not have such favorable binding poses for Michael addition through CDOCKER results, indicating that they have fewer chances to form covalent bonds with HER2 T798I mutant. NSC718305 displayed hydrogen bonding interactions with Lys753, Ser783, Asp863, Phe864 and hydrophobic interactions with Val734, Ala751, Leu796, Leu852 in the active site of HER2 T798I mutant. It also formed pi-sulfur interaction with Cys805 residues in the active site of HER2 T798I mutant (Figure 8(c)). Finally, HER2 T798I-NSC718305 docking complex was subjected to further MD simulations to estimate its binding stability.

For the HER2 T798M mutant, NSC659505 (−60.220 kcal/mol), NSC692910 (−59.838 kcal/mol) and NSC718305 (−66.841 kcal/mol) all had lower CDOCKER interaction energies than compound **19** (−59.719 kcal/mol) (Table 2). From visual inspection, the distance between Michael acceptor of NSC718305 and Cys805 of HER2 T798M mutant was about 4.4 Å (Figure 7(d)), which strongly suggests that NSC718305 can execute Michael addition with HER2 T798M mutant. However, no such favorable binding poses for Michael addition were observed for both NSC659505 and NSC692910 through CDOCKER, which reveals that they have fewer chances to form covalent bonds with HER2 T798M mutants. NSC718305 also bound in the active site of HER2 T798M mutant by forming hydrogen interactions with Lys753, Asp863, Gly865 and hydrophobic interactions with Ala751, Leu796, Met798, Cys805, Arg849 (Figure 8(d)). Finally, HER2 T798M-NSC718305 docking complex was subjected to further MD simulations to estimate its binding stability.

3.3. MD Simulations

Molecular dynamics (MD) simulation is an accurate method for investigating the physical movements of proteins-ligand complexes, giving a view of the dynamical evolution of the binding processes. In this study, HER2 L755S-NSC278329, HER2 L755S-NSC642003, HER2 T798I-NSC718305 and HER2 T798M-NSC718305 docking complexes were subjected to 50 ns MD simulations in an explicit hydration environment to investigate their binding stabilities. The dynamic stabilities and MD simulation trajectories of these complexes were analyzed by their backbone root mean square deviations (RMSD) [40]. Small RMSD values along with small fluctuations during the entire MD courses represent a stable binding system. As shown in Figure 9, HER2 L755S-NSC278329, HER2 L755S-NSC642003, HER2 T798I-NSC718305 and T798M-NSC718305 protein-ligand systems all reached the converged stage in the last 10 ns, with average RMSD values of 2.143 Å, 2.15 Å, 2.054 Å and 2.338 Å, respectively. Based on their favorable binding poses and stable RMSD values, NSC278329, NSC642003, NSC718305 were considered to have stable binding modes in these HER2 mutants.

3.4. ADMET Analysis

ADMET properties were calculated to investigate the pharmacokinetics of a prospective drug compound in the human body [41]. In this study, NSC278329, NSC642003 and NSC718305 were subjected to ADMET prediction using admet SAR and then compared to the FDA approved HER2 inhibitor, lapatinib. For absorption, all of these three compounds showed good human intestinal absorption (HIA), which suggests good oral delivery possibility. In the toxicity predictions, lapatinib, NSC278329 and NSC718305 are non-mutagenic (AMES toxicity test) and non-carcinogenic (carcinogenic profile) (Table 3) [42]. Since the US Food and Drug Administration (FDA) published the first *in vitro* *in vivo* drug interaction guidance

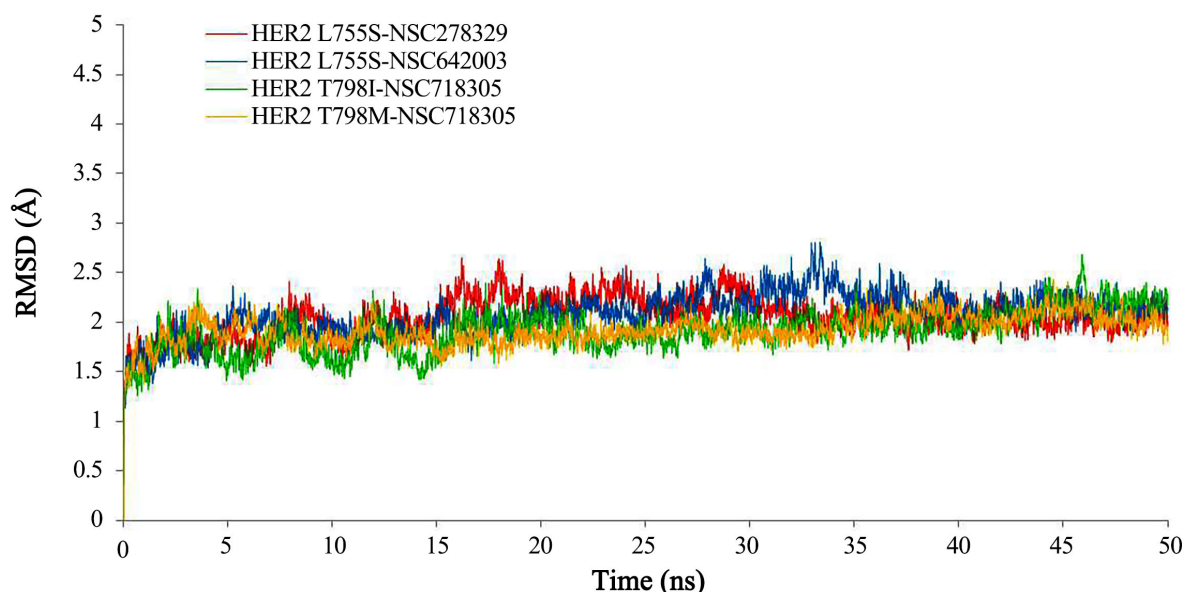


Figure 9. The root-mean-square deviation (RMSD) plots during the 50 ns MD simulation course for L755S-NSC278329 (red), HER2 L755S-NSC642003 (blue), HER2 T798I-NSC718305 (green) and HER2 T798M-NSC718305 (yellow).

Table 3. ADMET analysis of the screened compounds by admetSAR Server.

Parameter	Lapatinib	NSC278329	NSC642003	NSC718305
Human Intestinal Absorption	HIA+	HIA+	HIA+	HIA+
Blood-Brain Barrier	BBB+	BBB-	BBB-	BBB+
Caco-2 Permeability	Caco2-	Caco2-	Caco2-	Caco2-
P-glycoprotein Substrate	Substrate	Substrate	Non-substrate	Non-substrate
Renal organic cation transporter	Non-inhibitor	Non-inhibitor	Non-inhibitor	Non-inhibitor
CYP450 2C9 Substrate	Non-substrate	Non-substrate	Non-substrate	Non-substrate
CYP450 2D6 Substrate	Non-substrate	Non-substrate	Non-substrate	Non-substrate
CYP450 3A4 Substrate	Substrate	Substrate	Substrate	Substrate
CYP450 1A2 Inhibitor	Non-inhibitor	Non-inhibitor	Non-inhibitor	Non-inhibitor
CYP450 2C9 Inhibitor	Non-inhibitor	Non-inhibitor	Non-inhibitor	Non-inhibitor
CYP450 2D6 Inhibitor	Non-inhibitor	Non-inhibitor	Non-inhibitor	Non-inhibitor
CYP450 2C19 Inhibitor	Non-inhibitor	Inhibitor	Inhibitor	Non-inhibitor
CYP450 3A4 Inhibitor	Inhibitor	Inhibitor	Non-inhibitor	Inhibitor
CYP450 Inhibitory Promiscuity	High	Low	High	Low
hERG inhibition I	Inhibitor	Non-inhibitor	Non-inhibitor	Non-inhibitor
hERG inhibition II	Inhibitor	Non-inhibitor	Non-inhibitor	Non-inhibitor
AMES Toxicity	Non-toxic	Non-toxic	Non-toxic	Non-toxic
Carcinogens ^a	Non-carcinogens	Non-carcinogens	Carcinogens	Non-carcinogens

documents in 1997 and 1999, respectively, off-target transporter interactions and drug-drug interactions have been considered as the important criteria for drug development [43]. In human heart, hERG potassium channels are essential for regulating electrical activity [44]. According to the literature, the inhibition of human Ether-à-go-go-Related Gene (hERG) potassium channel may result in Long QT syndrome (LQTS), which is known as the lethal side effects in clinical studies [45]. The results of hERG prediction I/II showed that NSC278329, NSC642003 and NSC718305 are non-hERG inhibitors, suggesting that they have lower risk of causing LQTS than that of lapatinib. CYP450 enzymes-based unanticipated DDIs and drug metabolism problems are also a common cause of adverse drug events (ADE) [43]. According to our prediction, all of these three compounds can penetrate the pathway, which is regulated by CYP3A4 enzyme, suggesting that they may compete with other drugs. Furthermore, both NSC278329 and NSC718305 can inhibit CYP3A4 enzyme, which reveals that they can affect the metabolism of other drugs using the same CYP3A4 pathway, which is correlated to the function of platelet in human. NSC278329 and NSC642003 were predicted to inhibit CYP2C19 enzyme, suggesting that they can affect the function of platelet and should be carefully used. Compared tolapatinib, both NSC278329 and NSC718305 showed lower CYP inhibitory promiscuity inhibition, indicating that they have lower risks of causing CYP450 enzymes-based unanticipated drug-drug interactions and metabolism problems [46]. Overall, both NSC278329 and NSC718305 showed better ADMET properties than lapatinib.

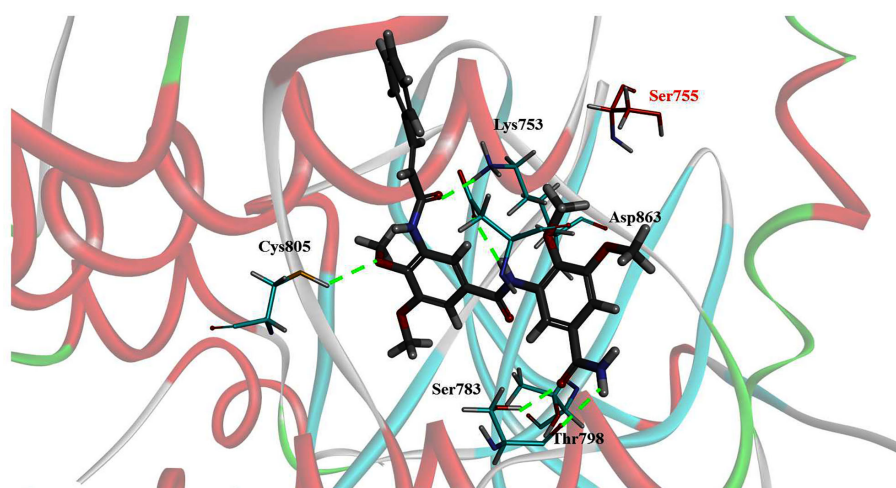
3.5. Evaluation of Hit Compounds

Cross docking analysis was performed to gain a deeper insight into the specificity of these selected irreversible HER2 inhibitors. In this study, NSC718305 was docked into HER2 L755S mutant while NSC278329 was docked into HER2 T798I and HER2 T798M mutants. Based on the results of cross docking, NSC718305 exhibited good CDOCKER scores of -71.664 kcal/mol by forming hydrogen bonding interactions with Lys753, Ser783, Cys805, Asp863 residues of HER2 L755S mutant (**Figure 10(a)**). On the other hand, NSC278329 exhibited strong binding with HER2 T798I mutant by forming hydrogen bonds with Lys753, Asn850, Thr862, Asp863, Gly865 residues (**Figure 10(b)**) with a good CDOCKER score of -70.482 kcal/mol. While docked into HER2 T798M mutant, NSC278329 formed hydrogen bonds with Lys753, Glu770, and Asp863 residues (**Figure 10(c)**) with a CDOCKER score of -66.760 kcal/mol. Therefore, both NSC278329 and NSC718305 were considered as potent irreversible inhibitors targeting HER2 L755S, T798I and T798M mutants.

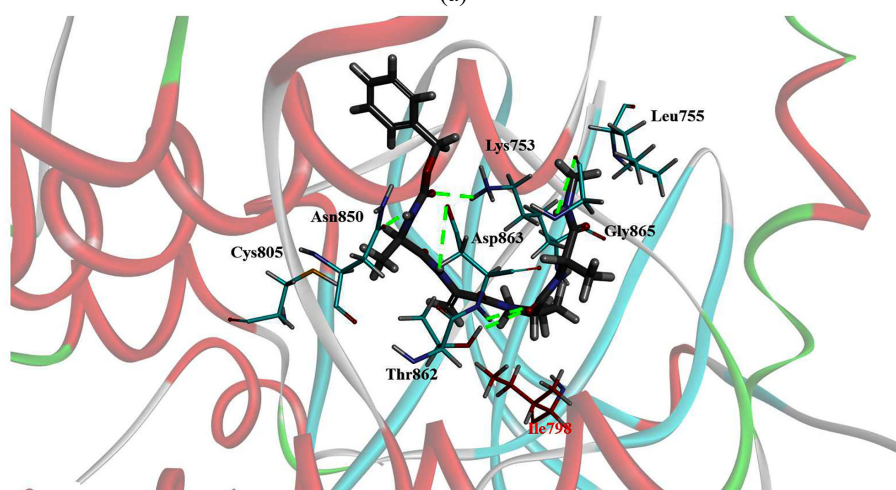
Interestingly, NSC718305 was the only compound to be screened by model II and model III. These two pharmacophore models totally differ from each other not only by the number of their features but also by their geographies. As shown in **Figure 11**, the docking conformations of NSC718305 in HER2 T798M mutant displayed completely different orientations and binding angles that in HER2 T798I mutant. Such different binding conformations may provide NSC718305 the possibility for mapping both pharmacophore models II and model III simultaneously.

4. CONCLUSIONS

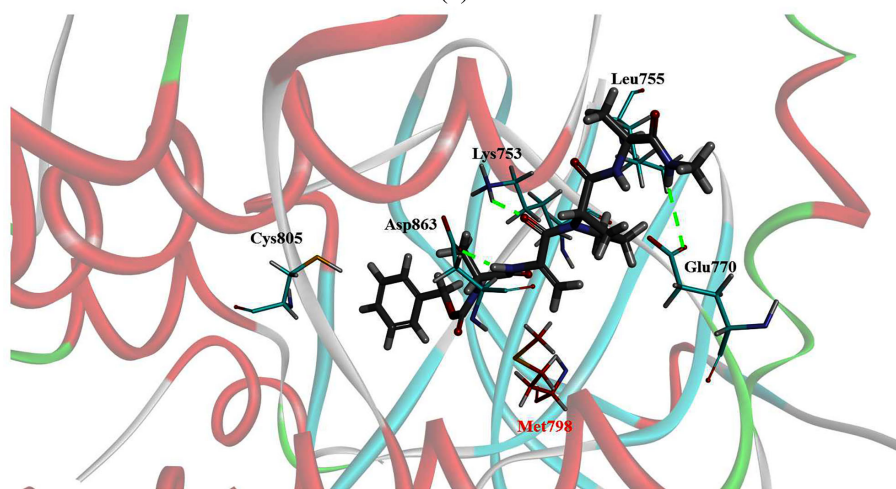
HER2 L755S, T798I and T798M point mutations were found to cause resistance toward FDA-approved lapatinib. Although several irreversible HER2 inhibitors have been synthesized to overcome such resistance problem, most of them were associated with lethal side effects, such as diarrhea, liver damage etc. Therefore, developing of novel irreversible HER2 inhibitors with less side effects and better ADMET properties against these HER2 mutants are highly desired. In this study, NSC278329 and NSC718305 were identified as novel irreversible HER2 inhibitors through a series of computational approaches. Unlike to the other experimental approaches, structure-based approach applied in this study has the advantages of searching compounds with novel structural scaffolds and desired chemical features. Furthermore, ADMET prediction adopted in this study has the ability to filter compounds with reasonable drug properties to decrease the risks of lethal side effects, such as off-target transporter interactions, drug-drug interactions and toxicity. Through cross docking, NSC278329 and NSC718305 were



(a)



(b)



(c)

Figure 10. Docking poses of (a) HER2 L755S-NSC718305 (CDOCKER score of -71.664 kcal/mol), (b) HER2 T798I-NSC278329 (CDOCKER score of -70.482 kcal/mol) and (c) HER2 T798M-NSC278329 (CDOCKER score of -66.760 kcal/mol). For each complex, the green dashed lines represent hydrogen bonds.

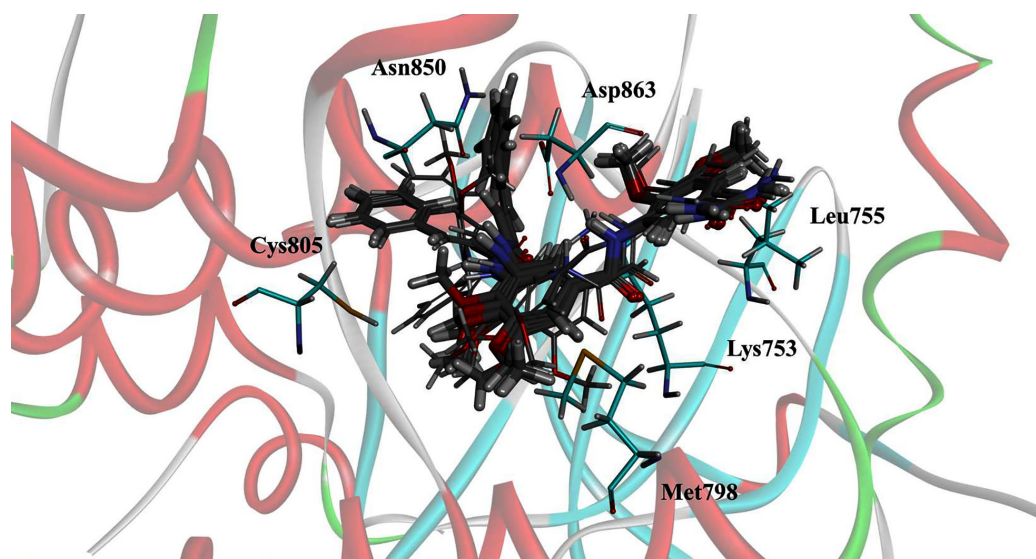


Figure 11. The superposition of the binding conformations of NSC7183005 towards HER2 T798M and HER2 T798I mutants.

proved to exhibit good binding interactions toward HER2 L755S, T798I and T798M mutants, suggesting they can extensively treat breast cancers with HER2 L755S, T798I and T798M mutants [47]. The above results strongly suggest that both NSC278329 and NSC718305 can be subjected for further *in vitro* *in vivo* studies as lead compounds for the development of better irreversible HER2 inhibitors through chemical modifications.

ACKNOWLEDGEMENTS

The authors greatly thank the Ministry of Science and Technology (MOST 103-2221-E-027-0901-MY3 and MOST 104-2221-E-027-073-MY3) and National Taipei University of Technology and Taipei Medical University (NTUT-TMU-101-10 and NTUT-TMU-102-10) for their financial supports.

CONFLICTS OF INTEREST

The authors declare no conflicts of interest regarding the publication of this paper.

REFERENCES

- Bellmunt, J., Werner, L., Bamias, A., Fay, A.P., Park, R.S., Riester, M., Selvarajah, S., Barletta, J.A., Berman, D.M., Muga, S.D., Salido, M., Gallardo, E., Rojo, F., Guancial, E.A., Bambury, R., Mullane, S.A., Choueiri, T.K., Loda, M., Stack, E. and Rosenberg, J. (2015) HER2 as a Target in Invasive Urothelial Carcinoma. *Cancer Medicine*, **4**, 844-852. <https://doi.org/10.1002/cam4.432>
- Logan, G.J., Dabbs, D.J., Lucas, P.C., *et al.* (2015) Molecular Drivers of Lobular Carcinoma *in Situ*. *Breast Cancer Research*, **17**, 76. <https://doi.org/10.1186/s13058-015-0580-5>
- Slamon, D.J., Clark, G.M., Wong, S.G., Levin, W.J., Ullrich, A., *et al.* (1987) Human Breast Cancer: Correlation of Relapse and Survival with Amplification of the HER-2/Neu Oncogene. *Science*, **235**, 177-182. <https://doi.org/10.1126/science.3798106>
- Brandt-Rauf, P.W., Pincus, M.R. and Carney, W.P. (1994) The *c-erbB-2* Protein in Oncogenesis: Molecular Structure to Molecular Epidemiology. *Critical Reviews in Oncogenesis*, **5**, 313-329.

<https://doi.org/10.1615/CritRevOncog.v5.i2-3.100>

5. Sun, A., Shi, Y., Shen, Y., Cao, L., Zhang, W. and Guan, X. (2015) Analysis of Different HER-2 Mutations in Breast Cancer Progression and Drug Resistance. *Journal of Cellular and Molecular Medicine*, **19**, 2691-2701. <https://doi.org/10.1111/jcmm.12662>
6. Burris, H.A. (2004) Dual Kinase Inhibition in the Treatment of Breast Cancer: Initial Experience with the EGFR/ErbB-2 Inhibitor Lapatinib. *The Oncologist*, **9**, 10-15. https://doi.org/10.1634/theoncologist.9-suppl_3-10
7. Minami, Y., Shimamura, T., Shah, K., La Framboise, T., Glatt, K.A., Liniker, E., *et al.* (2007) The Major Lung Cancer-Derived Mutants of ERBB2 Are Oncogenic and Are Associated with Sensitivity to the Irreversible EGFR/ERBB2 Inhibitor HKI-272. *Oncogene*, **26**, 5023-5027. <https://doi.org/10.1038/sj.onc.1210292>
8. Kancha, R.K., Bubnoff, N.V., Bartosch, N., Peschel, C., Engh, R.A. and Duyster, J. (2011) Differential Sensitivity of ERBB2 Kinase Domain Mutations towards Lapatinib. *PLoS ONE*, **6**, e26760. <https://doi.org/10.1371/journal.pone.0026760>
9. Rexer, B.N., Ghosh, R., Narasanna, A., Estrada, M.V., Chakrabarty, A., Song, Y., Engelman, J.A. and Arteaga, C.L. (2013) Human Breast Cancer Cells Harboring a Gatekeeper T798M Mutation in HER2 Overexpress EGFR Ligands and Are Sensitive to Dual Inhibition of EGFR and HER2. *American Association for Cancer Research*, **19**, 5390-5401. <https://doi.org/10.1158/1078-0432.CCR-13-1038>
10. Bose, R., Kavuri, S.M., Searleman, A.C., Shen, W., Shen, D., Koboldt, D.C., Monsey, J., Goel, N., Aronson, A.B., Li, S., Ma, C.X., Ding, L., Mardis, E.R. and Ellis, M.J. (2013) Activating HER2 Mutations in HER2 Gene Amplification Negative Breast Cancer. *Cancer Discovery*, **3**, 224-237. <https://doi.org/10.1158/2159-8290.CD-12-0349>
11. Mishra, R., Hanker, A.B. and Garrett, J.T. (2017) Genomic Alterations of ERBB Receptors in Cancer: Clinical Implications. *Oncotarget*, **8**, 114371-114392. <https://doi.org/10.18632/oncotarget.22825>
12. Li, D., Ambrogio, L., Shimamura, T., Kubo, S., Takahashi, M., Chirieac, L.R., Padera, R.F., Shapiro, G.I., Baum, A., Himmelsbach, F., Rettig, W.J., Meyerson, M., Solca, F., Greulich, H. and Wong, K.K. (2008) BIBW2992, an Irreversible EGFR/HER2 Inhibitor Highly Effective in Preclinical Lung Cancer Models. *Oncogene*, **27**, 4702-4711. <https://doi.org/10.1038/onc.2008.109>
13. Xie, H., Lin, L., Tong, L., Jiang, Y., Zheng, M., Chen, Z., Jiang, X., *et al.* (2011) AST1306, A Novel Irreversible Inhibitor of the Epidermal Growth Factor Receptor 1 and 2, Exhibits Antitumor Activity Both *in Vitro* and *in Vivo*. *PLoS ONE*, **6**, e21487. <https://doi.org/10.1371/journal.pone.0021487>
14. Takeda, M. and Nakagawa, K. (2017) Toxicity Profile Epidermal Growth Factor Receptor Tyrosine Kinase Inhibitors in Patients with Epidermal Growth Factor Receptor Gene Mutation-Positive Lung Cancer (Review). *Molecular and Clinical Oncology*, **6**, 3-6. <https://doi.org/10.3892/mco.2016.1099>
15. Klutchko, S.R., Zhou, H.R., Winters, T., Tran, T.P., Bridges, A.J., Althaus, I.W., *et al.* (2006) Tyrosine Kinase Inhibitors. 19. 6-Alkynamides of 4-Anilinoquinazolines and 4-Anilinopyrido[3,4-*d*]Pyrimidines as Irreversible Inhibitors of the erbB Family of Tyrosine Kinase Receptors. *Journal of Medicinal Chemistry*, **49**, 1475-1485. <https://doi.org/10.1021/jm050936o>
16. Barf, T. and Kaptein, A. (2012) Irreversible Protein Kinase Inhibitors: Balancing the Benefits and Risks. *Journal of Medicinal Chemistry*, **55**, 6243-6262. <https://doi.org/10.1021/jm3003203>
17. Yoshida, Y., Ozawa, T., Yao, T.W., Shen, W., Brown, D., Parsa, T.A., Raizer, J.J., *et al.* (2014) NT113, a Pan-ERBB Inhibitor with High Brain Penetration, Inhibits the Growth of Glioblastoma Xenografts with *EGFR* Amplification. *Molecular Cancer Therapeutics*, **13**, 2919-2929. <https://doi.org/10.1158/1535-7163.MCT-14-0306>
18. Ahmed, M., Sadek, M.M., Abouzid, K.A. and Wang, F. (2013) *In Silico* Design: Extended Molecular Dynamic Simulations of New Series of Dually Acting Inhibitors against EGFR and HER2. *Journal of Molecular Graphics and Modelling*, **44**, 220-231. <https://doi.org/10.1016/j.jmgs.2013.06.004>
19. Gogoi, D., Baruah, V.J., Chaliha, A.K. and Buragohain, A.K. (2016) 3D Pharmacophore-Based Virtual Screen-

ing, Docking and Density Functional Theory Approach towards the Discovery of Novel Human Epidermal Growth Factor Receptor-2 (HER2) Inhibitors. *Journal of Theoretical Biology*, **411**, 68-80.

<https://doi.org/10.1016/j.jtbi.2016.09.016>

20. Lipinski, C.A., Lombardo, F., Dominy, B.W. and Feeney, P.J. (2001) Experimental and Computational Approaches to Estimate Solubility and Permeability in Drug Discovery and Development Settings. *Advanced Drug Delivery Reviews*, **46**, 3-26. [https://doi.org/10.1016/S0169-409X\(00\)00129-0](https://doi.org/10.1016/S0169-409X(00)00129-0)
21. Veber, D.F., Johnson, S.R., Cheng, H.Y., Smith, B.R., Ward, K.W. and Kopple, K.D. (2002) Molecular Properties That Influence the Oral Bioavailability of Drug Candidates. *Journal of Medicinal Chemistry*, **45**, 2615-2623. <https://doi.org/10.1021/jm020017n>
22. Tian, S., Wang, J., Li, Y., Li, D., Xu, L. and Hou, T. (2015) The Application of *in Silico* Drug Likeness Predictions Pharmaceutical Research. *Advanced Drug Delivery Review*, **86**, 2-10. <https://doi.org/10.1016/j.addr.2015.01.009>
23. Zou, Y., Xiao, J., Tu, Z., Zhang, Y., Yao, K., Luo, M., Ding, K., *et al.* (2016) Structure-Based Discovery of Novel 4,5,6-Trisubstituted Pyrimidines as Potent Covalent Bruton's Tyrosine Kinase Inhibitors. *Bioorganic and Medicinal Chemistry Letters*, **26**, 3052-3059. <https://doi.org/10.1016/j.bmcl.2016.05.014>
24. Abraham, M.J., Murtola, T., Schulz, R., Páll, S., Smith, J.C., Hess, B., *et al.* (2015) GROMACS: High Performance Molecular Simulations through Multi-Level Parallelism from Laptops to Supercomputers. *SoftwareX*, **1-2**, 19-25. <https://doi.org/10.1016/j.softx.2015.06.001>
25. Berendsen, H.J.C., Vanderspoel, D. and Vandrunen, R. (1995) GROMACS: A Message-Passing Parallel Molecular Dynamics Implementation. *Computer Physics Communications*, **91**, 43-56. [https://doi.org/10.1016/0010-4655\(95\)00042-E](https://doi.org/10.1016/0010-4655(95)00042-E)
26. Lindorff-Larsen, K., Piana, S., Palmo, K., Maragakis, P., Klepeis, J.L., Dror, R.O., *et al.* (2010) Improved Side-Chain Torsion Potentials for the Amber ff99SB Protein Force Field. *Proteins-Structure Function and Bioinformatics*, **78**, 1950-1958. <https://doi.org/10.1002/prot.22711>
27. Case, D.A., Cerutti, D.S., III, T.E.C., Darden, T.A., Duke, R.E, T.J., *et al.* (2017) AMBER16 and AmberTools17. University of California, San Francisco.
28. Wang, J.M., Wolf, R.M., Caldwell, J.W., Kollman, P.A. and Case, D.A. (2004) Development and Testing of a General Amber Force Field. *Journal of Computational Chemistry*, **25**, 1157-1174. <https://doi.org/10.1002/jcc.20035>
29. Cheng, F., Li, W., Zhou, Y., *et al.* (2012) admetSAR: A Comprehensive Source and Free Tool for Assessment of Chemical ADMET Properties. *Journal of Chemical Information and Modeling*, **52**, 3099-3105. <https://doi.org/10.1021/ci300367a>
30. Levit, A., Yarnitzky, T., Wiener, A., Meidan, R. and Niv, M.Y. (2011) Modeling of Human Prokineticin Receptors: Interaction with Novel Small-Molecule Binders and Potential Off-Target Drugs. *PLoS ONE*, **6**, e27990. <https://doi.org/10.1371/journal.pone.0027990>
31. Vyas, V.K., Goel, A., Ghate, M. and Patel, P. (2015) Ligand and Structure-Based Approaches for the Identification of SIRT1 Activators. *Chemico-Biological Interactions*, **228**, 9-17. <https://doi.org/10.1016/j.cbi.2015.01.001>
32. Güner, O.F. and Henry, D.R. (2000) Metric for Analyzing Hit Lists and Pharmacophores. In: Güner, O.F., Ed., *IUL Biotechnology Series*, 191-212.
33. Güner, O.F., Waldman, M., Hoffmann, D. and Kim, J.H. (2000) Strategies for Database Mining and Pharmacophore Development, 1st Edition. In: Güner, O.F., Ed., *Pharmacophore Perception, Development, and Use in Drug Design, IUL Biotechnology Series*, 213-236.
34. Kumar, S.P. and Jha, P.C. (2016) Multi-level Structure-Based Pharmacophore Modelling of Caspase-3-

Non-Peptide Complexes: Extracting Essential Pharmacophore Features and Its Application to Virtual Screening. *Chemico-Biological Interactions*, **254**, 207-220. <https://doi.org/10.1016/j.cbi.2016.06.011>

35. Lu, S.H., Wu, J.W., Liu, H.I., Zhao, J.H., Liu, K.T., Chuang, C.K., Lin, H.Y., Tsai, W.B. and Ho, Y. (2011) The Discovery of Potential Acetylcholinesterase Inhibitors: A Combination of Pharmacophore Modeling, Virtual Screening, and Molecular Docking Studies. *Journal of Biomedical Science*, **18**, Article ID: 23244. <https://doi.org/10.1186/1423-0127-18-8>
36. Thangapandian, S., John, S., Sakkiah, S. and Lee, K.W. (2010) Ligand and Structure Based Pharmacophore Modeling to Facilitate Novel Histone Deacetylase 8 Inhibitor Design. *European Journal of Medicinal Chemistry*, **45**, 4409-4417. <https://doi.org/10.1016/j.ejmech.2010.06.024>
37. Ferla, M.P. and Patrick, W.M. (2014) Bacterial Methionine Biosynthesis. *Microbiology*, **160**, 1571-1584. <https://doi.org/10.1099/mic.0.077826-0>
38. Swellmeen, L., Shahin, R., Al-Hiari, Y., Alamiri, A., Hasan, A. and Shaheen, O. (2017) Structure-Based Drug Design of Pim-1 Kinase Followed by Pharmacophore Guided Synthesis of Quinolone-Based Inhibitors. *Bioorganic and Medicinal Chemistry*, **25**, 4855-4875. <https://doi.org/10.1016/j.bmc.2017.07.036>
39. Liu, C., He, G., Jiang, Q., Han, B. and Peng, C. (2013) Novel Hybrid Virtual Screening Protocol Based on Molecular Docking and Structure-Based Pharmacophore for Discovery of Methionyl-tRNA Synthetase Inhibitors as Antibacterial Agents. *International Journal of Molecular Sciences*, **14**, 14225-14239. <https://doi.org/10.3390/ijms140714225>
40. Telesco, S.E. and Radhakrishnan, R. (2009) Atomistic Insights into Regulatory Mechanisms of the HER2 Tyrosine Kinase Domain: A Molecular Dynamics Study. *Biophysical Journal*, **96**, 2321-2334. <https://doi.org/10.1016/j.bpj.2008.12.3912>
41. Schuler, M., Awada, A., Harter, P., Canon, J.L., Possinger, K., Schmidt, M., *et al.* (2012) A Phase II Trial to Assess Efficacy and Safety to Afatinib in Extensively Pretreated Patients with HER2-Negative Metastatic Breast Cancer. *B Breast Cancer Research and Treatment*, **134**, 1149-1159. <https://doi.org/10.1007/s10549-012-2126-1>
42. Tamokou, J.D.E. and Kuete, V. (2014) Chap. 10. Mutagenicity and Carcinogenicity of African Medicinal Plants. In: Kuete, V., Ed., *Toxicological Survey of African Medicinal Plants*, Elsevier, Amsterdam, 277-322. <https://doi.org/10.1016/B978-0-12-800018-2.00010-8>
43. Huang, S.M., Strong, J.M., Zhang, L., Reynolds, K.S., Nallani, S., Temple, R., *et al.* (2008) New Era in Drug Interaction Evaluation: US Food and Drug Administration Update on CYP Enzymes, Transporters, and the Guidance Process. *Journal of Clinical Pharmacology*, **48**, 662-670. <https://doi.org/10.1177/0091270007312153>
44. Sanguinetti, M.C. and Tristani-Firouzi, M. (2006) hERG Potassium Channels and Cardiac Arrhythmia. *Nature*, **440**, 463-469. <https://doi.org/10.1038/nature04710>
45. Wang, S., Li, Y., Wang, J., Chen, L., Zhang, L., Yu, H. and Hou, T. (2012) ADMET Evaluation in Drug Discovery. 12. Development of Binary Classification Models for Prediction of hERG Potassium Channel Blockage. *Molecular Pharmaceutics*, **9**, 996-1010. <https://doi.org/10.1021/mp300023x>
46. Guengerich, F.P. (2008) Cytochrome P450 and Chemical Toxicology. *Chemical Research in Toxicology*, **21**, 70-83. <https://doi.org/10.1021/tx700079z>
47. Tsou, H.R., Mamuya, N., Johnson, B.D., Reich, M.F., Gruber, B.C., Ye, F., *et al.* (2001) 6-Substituted-4-(3-Bromophenylamino)Quinazolines as Putative Irreversible Inhibitors of the Epidermal Growth Factor Receptor (EGFR) and Human Epidermal Growth Factor Receptor (HER-2) Tyrosine Kinases with Enhanced Antitumor Activity. *Journal of Medicinal Chemistry*, **44**, 2719-2734. <https://doi.org/10.1021/jm0005555>